

# A 64×64 1200fps CMOS Ion-Image Sensor with Suppressed Fixed-Pattern-Noise for Accurate High-throughput DNA Sequencing

Xiwei Huang, Fei Wang, Jing Guo, Mei Yan, Hao Yu\*, and Kiat Seng Yeo  
School of Electrical and Electronic Engineering, Nanyang Technological University, Singapore

## Abstract

A 64×64 CMOS ion-image sensor is demonstrated towards accurate high-throughput DNA sequencing. Dual-mode (pH/image) sensing is performed with ion-sensitive field-effect transistor (ISFET) fabricated in standard CMOS image sensor (CIS) process. After addressing physical locations of DNA slices by optical contact imaging, local pH for one DNA slice can be mapped to its physical address with accurate correlation. Moreover, pixel-to-pixel ISFET threshold voltage mismatch is reduced by correlated double sampling (CDS) readout. Measurements show a sensitivity of 103.8mV/pH and fixed-pattern-noise (FPN) reduction from 4% to 0.3% with speed of 1200fps.

**Keywords:** CIS, ISFET, pH detection, contact imaging, CDS, DNA sequencing

## Introduction

ISFET utilizing the top most passivation layer ( $\text{Si}_3\text{N}_4$ ) in standard CMOS process for ion sensing has drawn great attention recently [1-7]. One emerging application is to detect  $\text{H}^+$  (or pH) released by DNA polymerase synthesis during sequencing [1-2]. A long DNA chain is first fragmented into slices and clonally amplified onto reaction carrier, i.e., microbeads, which are distributed into microwell array on ISFET sensor. Then the measured pH change for one DNA slice at a microbead indicates the relevant DNA sequence of ATCG [1]. When the pH changes for DNA slices are detected at millions of spatially localized microbeads by large-arrayed ISFET sensor, high-throughput and label-free DNA sequencing can be realized. However, there are still significant false sequencing data reported. Firstly, local pH response needs to be correlated to the physical location that contains one microbead. If there is no microbead in a microwell, the reported pH response is false due to cross-talk from neighboring microbeads. Secondly, pH variation of large-arrayed ISFET sensor exists due to pixel-to-pixel threshold voltage  $V_T$  mismatch, or fixed pattern noise (FPN).

## Implementation

In this paper, a 64×64 ion-image sensor array in standard CIS process is demonstrated. As shown in Fig. 1 and 2, each pixel contains a 4T-CIS pixel to sense the optical image of microbead by contact imaging [8]; meanwhile, source follower (SF) can work as ISFET to detect pH value at one microbead. Photodiode (PD) first collects photons and converts them to electrons, which are transferred to floating diffusion (FD) by turning on 'TX'. The corresponding voltage signal for optical image is read out through the source of SF. In addition, the poly-gate of SF is connected to the top metal/passivation layer, acting as ion-sensitive membrane of ISFET. Since the change of ion ( $\text{H}^+$ ) concentration (or pH) can cause proportional  $V_T$  change of the SF, the corresponding voltage signal for pH value is read out through the source of SF as well.

As shown in Fig. 2, each pixel output voltage after readout is further digitized through column S/H, global amplifier and pipelined ADC. The pixel array readout is controlled by row and column decoder. With column S/H, the pixel output voltage is amplified by switched-capacitor amplifier with gain

$C_S/C_F$  selected among (1X, 2X, 4X), which is upon different input signal levels to improve sensitivity and dynamic range. The analog signal is then digitized by a 12-bit pipelined ADC. The row readout time is 13 $\mu\text{s}$  including sampling, amplification and digitization, which results in a frame rate of 1200fps for a 64×64 array.

The dual-mode ion-image sensor is operated with readout timing as follows. When reaction carrier microbeads attached with slices of DNA are loaded onto pixel array, the image mode is turned on by setting corresponding readout timing control in Fig. 3(a) as a normal 4T-CIS pixel. The shadow image of microbead can be captured by contact imaging [8]. As such, the existence of microbead at each pixel can be determined with address. Next, when the chemical mode is turned on by changing to chemical readout timing control as in Fig. 3(b), the pH value at one microbead is obtained within each pixel. As such, one can obtain the correlation between the measured pH data and the distribution of microbeads. The false pH data is thereby eliminated by the dual-mode sensor.

Furthermore, pixel-to-pixel  $V_T$  mismatch (or FPN) significantly affects the readout accuracy of large array. As shown in Fig. 2, switches 'ISFR'/'ISFS' are added to support correlated double sampling (CDS) for both CIS and ISFET readout. Note that CDS is applied to suppress pixel-to-pixel  $V_T$  mismatch by using each pixel itself as reference. As shown in Fig. 3, before loading solution with microbeads, 'RST' is turned on, and the reset voltage  $V_{\text{RST}}$  is stored at capacitor  $C_S$  by turning on 'SHR'. Meanwhile, 'ISFR' is turned on to force  $V_{\text{POS}} = V_{\text{CM}}$ , the common mode voltage. As such, the output  $V_{\text{OUT1}} = V_{\text{OUTP}} - V_{\text{OUTN}} = \alpha \cdot (C_S/C_F) \cdot (V_{\text{RST}} - V_{\text{CM}} + V_T)$ , where  $\alpha$  is the gain of the source follower. After loading solution with microbeads, 'ISFS' is turned on to force  $V_{\text{POR}} = V_{\text{CM}}$ . The output  $V_{\text{OUT2}} = V_{\text{OUTP}} - V_{\text{OUTN}} = \alpha \cdot (C_S/C_F) \cdot (V_{\text{REF}} - V_{\text{CM}} + V_T - dV)$ , where  $dV$  is the threshold voltage change caused by the chemical reaction between ion and the passivation layer. As a result, the difference  $V_{\text{OUT1}} - V_{\text{OUT2}} = \alpha \cdot (C_S/C_F) \cdot (V_{\text{RST}} - V_{\text{REF}} + dV)$  removes the dependence on  $V_T$ . The CDS readout can thereby largely reduce the  $V_T$  mismatch (or FPN).

## Measurement Results

The chip micrograph with architecture and testing system is shown in Fig. 4. The proposed dual-mode sensor is fabricated in TSMC 0.18 $\mu\text{m}$  CIS process, and packaged by liquid-friendly encapsulation with sensing area open. The design specifications are summarized in the table of Fig. 4.

The correlated contact image and pH map of microbeads are shown in Fig. 5. The contact image determines the existence of microbeads and provides their addressed distribution. The pH map is thereby locally associated with microbeads by filtering out those uncorrelated pH data. The pH measurement results are shown in Fig. 6. The pH of solution is changed by adding HCL and NaOH. The pH sensitivity of ISFET by CIS process is measured as 26.2mV/pH with amplifier gain=1 and as 103.8mV/pH with amplifier gain=4. The sensor chip is also calibrated by testing the pH change of a bacteria (*E. Coli*) culture solution at different time intervals. The measurement results by the dual-mode sensor can correlate well with one

commercial pH meter (Checker, Hanna Instruments, RI, US).

The comparison of readout voltage variations with and without CDS is shown in Fig. 7. After performing spatial FFT to the readout voltages with respect to the addresses of ISFET sensor array, the mean and peak variations are reduced by 0.17mV and 0.25mV, respectively. The FPN is accordingly reduced from 4% down to 0.3%. The comparison with the state-of-art ISFET sensors is summarized in Table I. The proposed dual-mode sensor shows the state-of-art results: 10 $\mu$ m pixel pitch, 64 $\times$ 64 pixel array, fast frame rate of 1200fps, and sensitivity of 103.8mV/pH in standard CIS process.

### References

- [1] J. M. Rothberg, et al., *Nature*, pp. 348-352, 2011.
- [2] C. Toumazou, et al., *Nature Methods*, pp. 641-646, 2013.
- [3] T. Hizawa, et al., *Sens. Actuat. B Chem.*, pp. 509-515, 2006.
- [4] M. J. Milgrew, et al., *Tech. Dig. of ISSCC*, pp.590-638, 2008.
- [5] B. Nemeth, et al., *Sens. Actuat. B Chem.*, pp.747-752, 2012.
- [6] W. P. Chan, et al., *J. Solid State Circuits*, pp.1923-1934, 2010.
- [7] A. Manickam, et al., *Tech. Dig. of VLSI Symp.*, pp.126-127, 2012.
- [8] R. R. Singh, et al., *J. Solid-State Circuits*, pp.2822-2833, 2012.

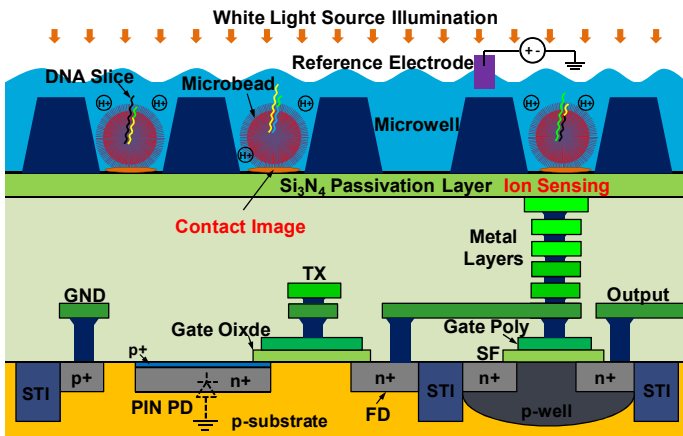


Fig. 1. Cross-section pixel layout of dual-mode sensor for DNA sequencing with microbead by contact imaging and ion sensing.

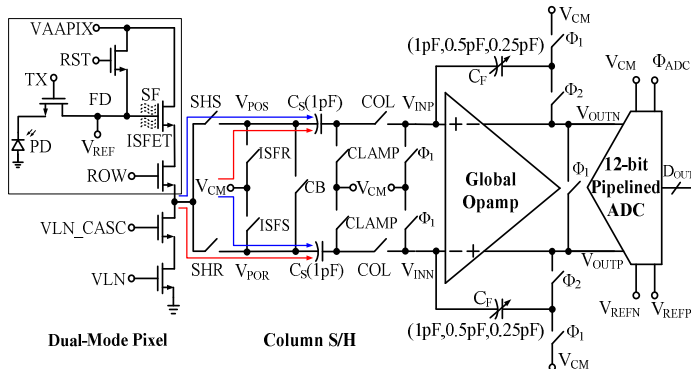


Fig. 2. Dual-mode sensor pixel and CDS readout schematic.

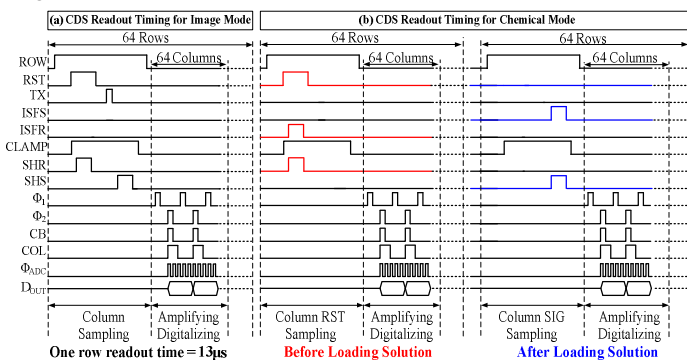


Fig. 3. CDS readout timing diagram (a) image mode (b) chemical mode.

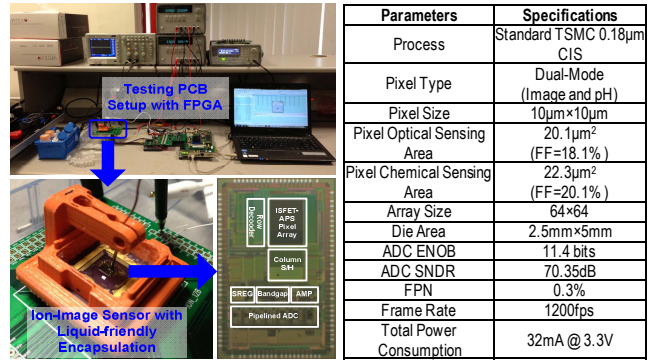


Fig. 4. Micrograph photo of the dual-mode sensor chip, testing setup and specifications.

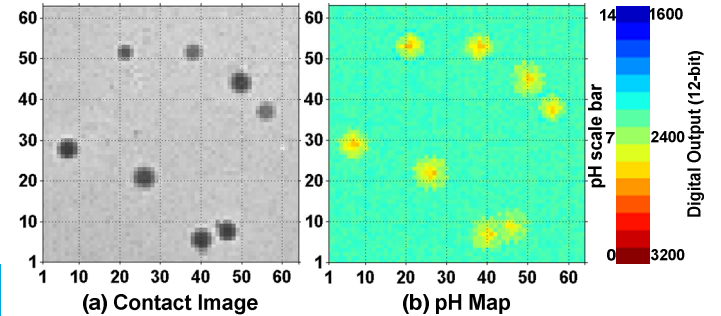


Fig. 5. The correlated maps of distributed microbeads: (a) contact images; and (b) pH values.

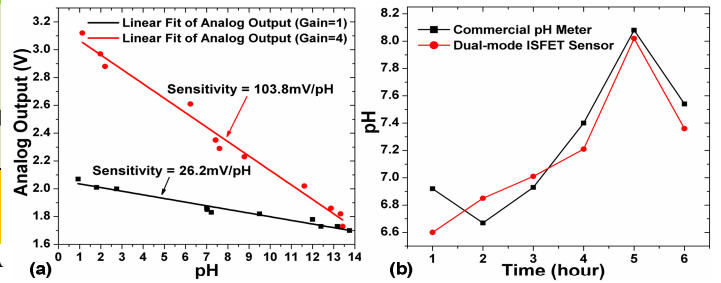


Fig. 6. Measurement results: (a) pH sensitivity of dual-mode ISFET sensor; and (b) the comparison with commercial pH meter for bacteria (*E. Coli*) culture solution with glucose at different time intervals.

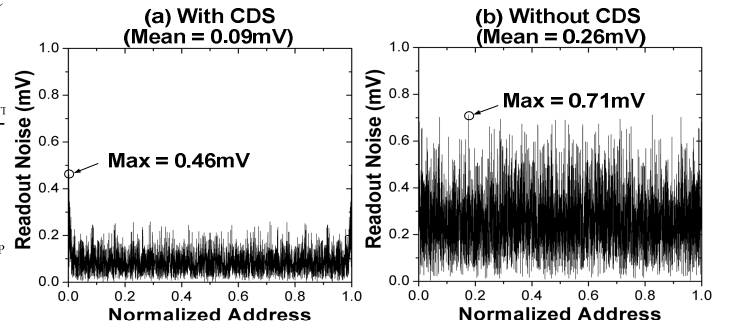


Fig. 7. Measurement results: spatial FFT of readout voltage variations (a) with CDS and (b) without CDS readout.

Table I. Comparison of state-of-art ISFET sensors

	[4]	[5]	[6]	[7]	This Work
Process	5 $\mu$ m Non-CMOS	0.35 $\mu$ m Modified CMOS	0.35 $\mu$ m Standard CMOS	0.18 $\mu$ m Standard CMOS	0.18 $\mu$ m Standard CMOS
Pixel Size	200 $\mu$ m $\times$ 200 $\mu$ m	12.8 $\mu$ m $\times$ 12.8 $\mu$ m	10.2 $\mu$ m $\times$ 10.2 $\mu$ m	20 $\mu$ m $\times$ 2 $\mu$ m	10 $\mu$ m $\times$ 10 $\mu$ m
Array Size	10 $\times$ 10	16 $\times$ 16	64 $\times$ 64	8 $\times$ 8	64 $\times$ 64
Frame Rate	30fps	-	100fps	-	1200fps
Sensitivity	229mV/pH	46mV/pH	20mV/pH	37mV/pH	26.2mV/pH (gain=1) 103.8mV/pH (gain=4)
Dual-Mode	No	No	No	No	Yes